ORIGINAL PAPER

Bony labyrinth shape differs distinctively between modern wolves and dogs

L. A. Janssens[1,2] · P. Gunz[3] · T. E. Stenger[4] · M. S. Fischer[4] · M. Boone[5] · A. Stoessel[3,4,6]

Abstract
Additional reliable anatomical markers are needed for differentiating archaeological wolves and dogs, to support clarifying the origin(s) of dogs. Candidate structures should have good potential to survive various taphonomic conditions. The petrous bone is one potential differentiating structure, and could be further useful when aDNA cannot be extracted otherwise. The petrous bone houses the bony labyrinth (semicircular canals, vestibule, and cochlea). Across a number of taxa, its intricate shape has been shown to carry indicator taxonomic information, supporting clear distinctions between and among mammalian groups. In this report, we explore the three-dimensional shape of the bony labyrinth of wolves and dogs, using micro-computed tomography and 3D geometric morphometrics. We examined 20 modern Eurasian wolves and 20 modern mesaticephalic dogs with comparable skull lengths. We show that dogs have on average a significantly smaller bony labyrinth than wolves. In shape space, wolves and dogs form significantly different, non-overlapping clusters with dogs having a larger relative size of the lateral semicircular canal, smaller relative size of the vertical canals and oval window, and shorter relative cochlea streamline length, with a more antero-ventrally tilted modiolus. These shape differences are not related to allometric effects. Results of this study warrant examination of preserved archaeological and paleo-ontological petrous bones from the oldest possible dogs and isopatric wolves.

Keywords Inner ear · Cochlea · Semicircular canals · Geometric morphometrics · Wolf · Dog · Domestication

L. A. Janssens and A. Stoessel contributed equally.

✉ L. A. Janssens
coati1@icloud.com

✉ A. Stoessel
alexander.stoessel@uni-jena.de

[1] Department of Archaeology, University of Leiden, Einsteinweg 2, 2333 CC Leiden, The Netherlands

[2] Department of Archaeology, University of Ghent, Sint-Pietersnieuwstraat 35, 9000 Ghent, Belgium

[3] Department of Human Evolution, Max Planck Institute for Evolutionary Anthropology, Deutscher Platz 6, 04103 Leipzig, Germany

[4] Institute of Zoology and Evolutionary Research, Friedrich Schiller University Jena, Erbertstraße 1, 07743 Jena, Germany

[5] Department of Physics and Astronomy, Centre for X-ray Tomography, Ghent University, Proeftuinstraat 86, 9000 Ghent, Belgium

[6] Department of Archaeogenetics, Max Planck Institute for the Science of Human History, Kahlaische Strasse 10, 07745 Jena, Germany

Introduction

Zoologists, geneticists, and archaeologists have been working to resolve the timing, location, and stimuli that surround the domestication of wolves. Eurasian wolves clearly are ancestors of domestic dogs, but the actual founding wolf population is not yet known. Pivotal questions that first must be resolved involve the ability to differentiate archaeological wolf and dog remains correctly. Factors that contribute negatively include fragmented, incomplete ancient specimens, and insufficient ancient DNA (aDNA) for study.

Many phenotypic traits that were proposed historically to differentiate wolves and dogs now have been rejected, based on new data and high-quality re-analysis of older data (Ameen et al. 2017; Drake et al. 2015, 2017; Drake and Klingenberg 2010; Janssens et al. 2016a, b, c, 2019). Traits that have remained valid for sub-speciation include dog size reduction; dog brain size ratio reduction; smaller dog P[4] mesiodistal diameter; small M1 mesiodistal diameter; large dog orbital angle; and wider dog snout width and skull height indices. However, one problem with these

remaining traits is that the oldest archaeological canine skulls mostly are incomplete, leaving only P^4 (if present) and relative size as possible differentiating criteria. Thus, the differences between valid species-differentiating canid traits and those that actually are available highlight a need for new anatomical diagnostics. The petrous bone is a potential candidate for development as a species-differentiating trait.

The petrous part of the temporal bone (Fig. 1) contains the bony labyrinth (anterior, lateral, posterior semicircular canals, vestibule, and cochlea), a complex structure that houses the organs of balance and hearing (Costeur et al. 2017; Jeffery and Spoor 2004). The petrous bone is the most-dense bone in the mammalian body (Lam et al. 2003), and it preserves well in fossil mammalian skeletal remains (Lam et al. 1999; Lyman 1984). In research to date, non-invasive microcomputed tomography (micro-CT) and geometric morphometric (GM) semi-landmark-based 3D shape analysis of the bony labyrinth have defined clear differentiations among

mammalian subspecies (Gunz et al. 2012) and even among populations (de León et al. 2018).

In a recent geometric morphometrics (GM) study of modern dogs, modern wolves, and archaeological dogs, using micro-CT imaging, bony labyrinth shape did not support a species-differentiating hypothesis (Schweizer et al. 2017). Actually, the study found substantial overlap between wolves and dogs. The shape of the bony labyrinth varied similarly among dogs and wolves, mostly generated allometrically as covariation of size and shape (Schweizer et al. 2017). Schweizer et al. (2017) had evaluated a thorough spectrum that included many modern dog breeds that spanned miniature, giant, chondrodystrophic, dolichocephalic, and brachycephalic types. They also evaluated several subspecies of non-Eurasian wolves (*C. l. chanco*; *C. l. arabs*; *C. l. lycaon*) that clearly are not ancestors of modern dogs (Aggarwal et al. 2007). Correlations between body size and morphology of the mammalian ear region have been previously shown (Nummela 1995; Lebrun et al. 2010; Spoor

Fig. 1 **a** Dorsal view of a dog skull with opened skull cap and inner view on the skull base. The right petrous bone is colored purple; **b** dorsal view of a wolf right petrous bone; **c** identical view with the bony structure made transparent, to show the position of the hollow bony labyrinth, colored purple; **d** lateral view of the right bony labyrinth, denuded from bone, showing the anterior (ASC), posterior (PSC) and lateral semicircular canal (LSC), cochlea and oval window
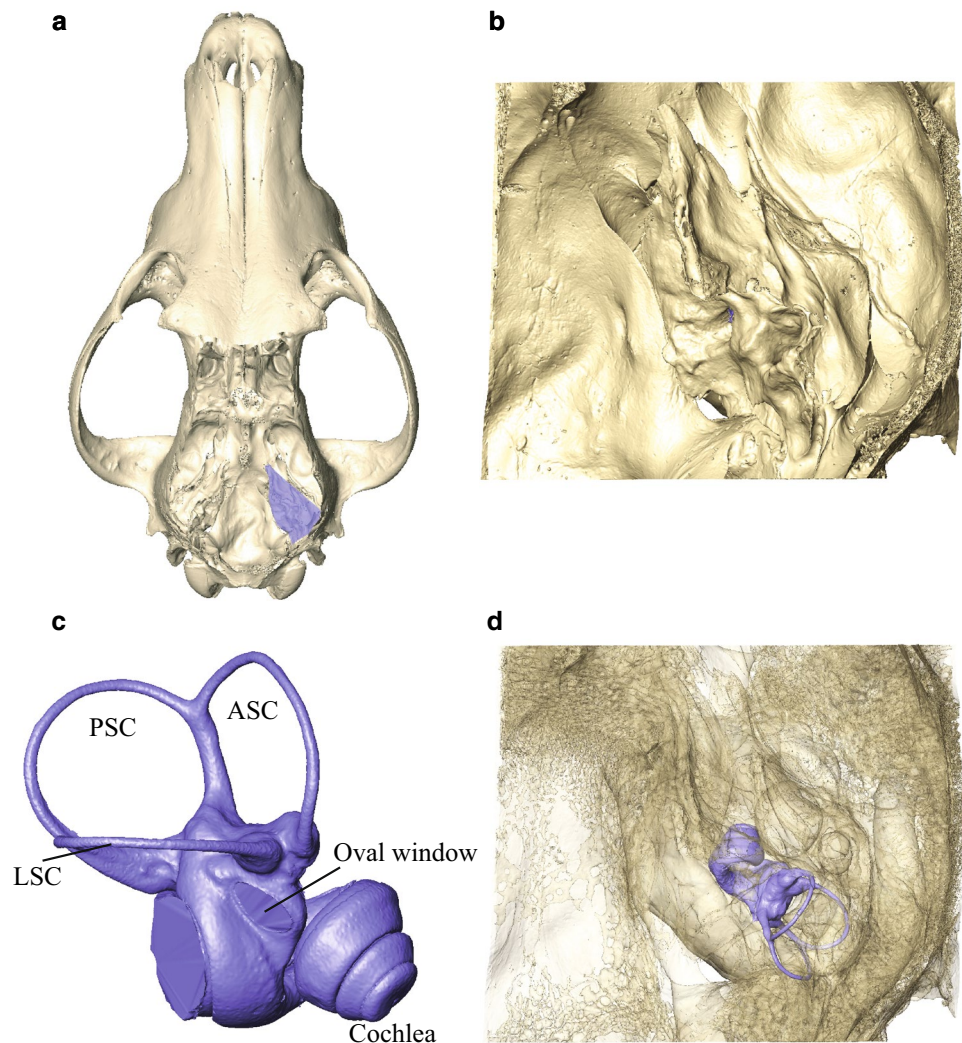
et al. 2007). Thus, despite evidently disappointing results from Schweizer et al. (2017), it is worth considering that allometric effects on bony labyrinth shape? (Lebrun et al. 2010; Alloing-Séguier et al. 2013), and more pronounced scaling-driven variance of overall shapes, may be important when considering groups of more diverse and broader body size ranges (Lebrun et al. 2010). If allometric effects obscure size-unrelated, subtle differences in labyrinth shape among dogs and wolves, species-relevant differences may not be obvious.

We hypothesize that allometric effects could obscure non-size-related, subtle differences in labyrinth shape. To test this hypothesis, we chose an alternative GM approach and minimized the effect of allometry by comparing modern adult wild wolves of Eurasian origin that are the probable ancestor type of dogs (Thalmann et al. 2013) with modern mesaticephalic dogs with comparable skull lengths. Mesaticephalic skulls have medium skull length and muzzle width (Slatter 2003) in all archaeological specimens, but vary from some modern dogs that have brachycephalic (pug) or dolichocephalic (borzoi) skulls, both reflecting modern gene pool isolation and thus not present in wild canids, ancient or modern.

Materials and methods

Study population and imaging

We analyzed dry skulls of 20 modern dogs and 20 Eurasian wolves. All specimens were adult modern wild wolves or adult modern mesaticephalic dogs with comparable skull length. The skulls were scanned using micro-CT systems with image spatial resolutions ranging between 0.024 and 0.050 mm. The total skull length was established according to Von den Driesch (1976), and detailed image spatial resolution for each of the specimen is given in Table 1.

All modern dog specimens were scanned using the custom-made HECTOR (Masschaele et al. 2013) scanner of the Ghent University Centre for X-ray Tomography (UGCT). The wolf specimens, curated at the Museum für Naturkunde in Berlin, Germany, were scanned using the custom-made diondo d3 microCT scanner at the MPI-EVA in Leipzig, Germany. Following the protocol of Gunz et al. (2012), micro-CT scan images were used to extract the 3D surfaces of the bony labyrinth using the 'Isosurface' module in Avizo™ 7.1 and 8.1 (Visualization Science Group). Our goal was to analyze bony labyrinths from the right side of the skull. However, in cases of destruction or fillings of the right side, the left labyrinth was reconstructed after mirror-imaging the original tiff stack. Based on a single threshold that best represents the surface of the bony labyrinth (selection of appropriate threshold done visually), the 'Isosurface'

Table 1 List of individual specimens used in this study

Group	Museum ID	Provenance/breed	Image-spatial resolution (mm)	Skull-length (mm)
Wolf	ZMB-22340	Central Asia	0.0274	245
Wolf	ZMB-48867	China	0.0274	250
Wolf	ZMB-16454	China	0.0238	240
Wolf	ZMB-93695	China	0.0238	245
Wolf	ZMB-83467	Europe/Russia	0.0238	250
Wolf	ZMB-93303	Europe/Russia	0.0256	255
Wolf	ZMB-52539	Europe/Russia	0.0256	245
Wolf	ZMB-2945	Europe/Russia	0.0256	250
Wolf	ZMB-83460	Europe/Russia	0.0256	250
Wolf	ZMB-29207	Europe/Russia	0.0256	255
Wolf	ZMB-29209	Europe/Russia	0.0256	260
Wolf	ZMB-52531	Europe/Russia	0.0256	275
Wolf	ZMB-28475	Europe/Russia	0.0256	235
Wolf	ZMB-29208	Europe/Russia	0.0247	250
Wolf	ZMB-30415	Europe/Russia	0.0238	255
Wolf	ZMB-22373	Europe/Russia	0.0238	250
Wolf	MAM-xxxx	Europe/Russia	0.0912	245
Wolf	ZMB-83466	Turkey	0.0256	250
Wolf	ZMB-56617	Turkey	0.0238	255
Wolf	ZMB-22350	Turkey	0.0238	250
Dog	A	Belgian shepherd	0.0499	231
Dog	B	German shepherd	0.0499	249
Dog	C	Irish setter	0.0499	256
Dog	D	Rhodesian ridgeback	0.0499	223
Dog	6232	Unknown	0.0499	274
Dog	6509	Belgian shepherd	0.0499	230
Dog	6512	Gordon Setter	0.0499	242
Dog	6566	Komondor	0.0499	230
Dog	6583	Irish wolfhound	0.0499	247
Dog	6689	Irish wolfhound	0.0499	264
Dog	6592	Bloodhound	0.0499	254
Dog	6655	Bloodhound	0.0499	250
Dog	6664	German shepherd	0.0499	242
Dog	6668	Irish wolfhound	0.0499	239
Dog	6684	Leonberger	0.0499	239
Dog	6589	Leonberger	0.0499	255
Dog	6764	Great dane	0.0499	252
Dog	6770	Canadian shepherd	0.0499	233
Dog	E	Bouvier des Flandres	0.0499	238
Dog	6608	German shepherd	0.0499	247

module calculates a 3D surface directly from the matrix of grey-scale voxels (needs homogenous filling of bony labyrinth). After removing all reconstructed adjacent structures not belonging directly to the bony labyrinth (using 'Surface

Editor'), surfaces were saved in STL format and imported into GEOMAGIC STUDIO™ 12-20 (Geomagic, Inc.) for surface closing and necessary smoothing. The subsequent measurement protocol for the digitization of landmark and semi-landmark coordinates followed an earlier protocol (Gunz et al. 2012; Gunz and Mitteroecker 2013), except for minor modifications (see below).

Quantification

Shape analysis of the bony labyrinth is based on evaluating a large number of landmarks and semi-landmarks. Landmarks were digitized using AVIZO™ 6.1–8.1. Processing of landmark coordinates was done using Mathematica™ (Wolfram Research, Inc.). The measurement protocol for obtaining landmark data was described previously (Gunz et al. 2012). The procedure involves placing 20 landmarks and approximately 280 semi-landmarks, beginning with computing a midline skeleton of the surface model by thinning the encased volume. This skeleton serves as a curvature template for placing midline landmarks of the semicircular canals and the common crus (Fig. 2). For the cochlea, we used a manually created midline skeleton. In addition to midline landmarks, a set of 'outline' measurement points were placed on the outer surface of each semicircular canal and the common crus, along a curve farthest away from the vestibule. To quantify shape of the oval window, another set of landmarks was placed along a curve on the margin of the oval window. Changes to the measuring protocol of Gunz et al. (2012) affected six landmarks (three on midline and three on outline) placed on the vestibular side of the ampullae of the three semicircular canals and defining the starting point of the curves of each of the three canals. Instead of placing these landmarks at the fusion of the ampulla to the vestibule, they were placed midmost of the ampulla midline skeleton (Fig. 2). On the outline, the landmark is defined

by the entry of the vestibular nerve into the bony ampulla. Another change affects the ending landmarks of the common crus that we placed in vestibular orientation, rather than aligning with the outline border of the vestibule (new template included as supporting information).

Bony labyrinth shape was analyzed using GM methods that require all specimens to have the same number of landmarks (coordinates) at corresponding locations. Therefore, curves along the midlines and the outlines of the semicircular canals, the oval window, and the midline of the cochlea, were provided with uniform semi-landmark numbers. Subsequently, semi-landmarks were allowed to slide along their respective curves to minimize the thin-plate spline bending energy between each specimen and the average shape (computed as the mean of all Procrustes coordinates). This sliding step ensures geometric correspondence of the semi-landmarks among individuals (Bookstein 1997; Gunz et al. 2005; Gunz and Mitteroecker 2013; Rohlf and Marcus 1993). The 3D landmark and slide semi-landmark data on the semicircular canals, the oval window, and the cochlea, were converted into shape variables using Generalized Least Squares Procrustes superimposition (Rohlf 1990). Procrustes superimposition standardizes position and orientation and also scales all specimens to unit centroid size.

Principal component analysis (PCA) was used to evaluate the Procrustes coordinates. Multivariate regression of the Procrustes shape coordinates on the natural logarithm of centroid size was used to study allometry (Gunz and Mitteroecker 2013). A permutation test (Good 2013), based on the Procrustes distance between group means, was computed to evaluate the statistical significance of shape differences among modern dogs and wolves. For this analysis, the length of the Procrustes distance between the two group averages, with average differences computed after randomly reshuffling group affiliations 5000 times, was compared (Mitteroecker and Gunz 2009). All data processing and statistical
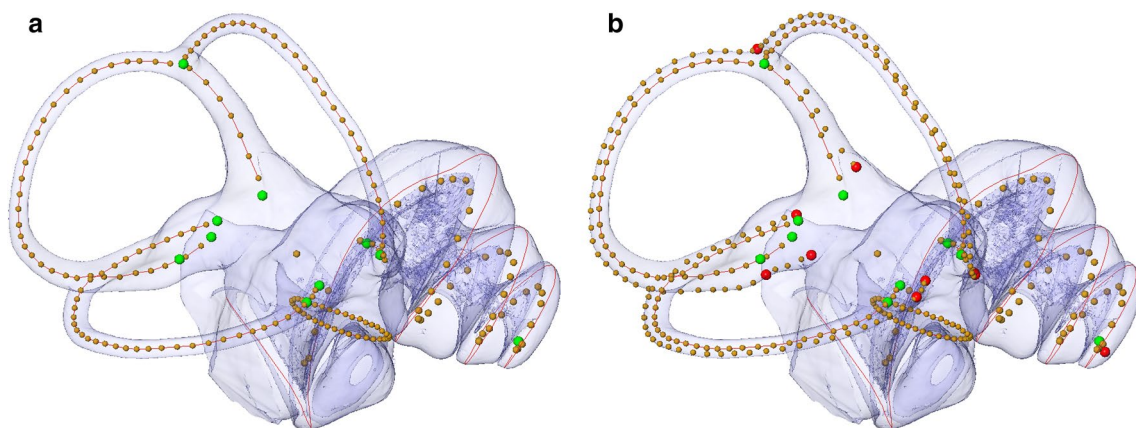
Fig. 2 Only midline (**a**) and midline and outline (**b**) set of landmarks (midline: green; outline: red) landmarks and semi-landmarks (orange) used for statistical shape analysis
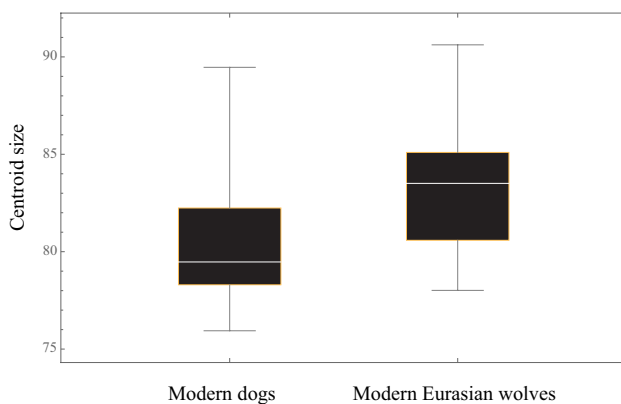
analyses were performed in Mathematica™ (Wolfram Research, Inc.), using software routines developed by PG and Philipp Mitteroecker (Gunz and Mitteroecker 2013).

Results

Total skull length in wolves (250 mm ± 8.1 mm) did not differ significantly ($p = 0.094$) from mesaticephalic dogs (245 mm ± 12.6 mm). Dogs and wolves overlap broadly in bony labyrinth size (Fig. 3), but mean centroid size of the landmark configuration in wolves is significantly larger ($p = 0.011$) than in dogs, implying slightly larger bony labyrinth in wolves, where skull length is comparable.

The first three principal components (PCs) of canine bony labyrinth shape explain 50% of the total variance. Shape space of the first three PCs reveals that wolves and dogs form non-overlapping clusters (Fig. 4) with mean shapes that differ significantly ($p < 0.001$). The main axis of separation between wolves and dogs is found along PC 1, explaining 24.8% of total variance (Figs. 4, 5). In contrast, dogs and wolves overlap broadly on PC 2 (15.4% of total sample variance) and PC 3 (10.1% of total sample variance). The variance of shape is similar between wolves (0.00276) and modern dogs (0.00286).

Allometry had a significant effect ($p < 0.001$) on distributions of shape variables over the entire study population, explaining 6.7% of the total variance. Scaling explains slightly more of the shape variance among modern dogs (11.4%) than wolves (10.1%), ($p < 0.001$). Centroid size correlates more strongly with PC 2 ($r = 0.543$, explaining 30% of variance) than with PC 1 ($r = -0.191$, explaining 4% of variance), with the latter defining the axis separating dogs from wolves.
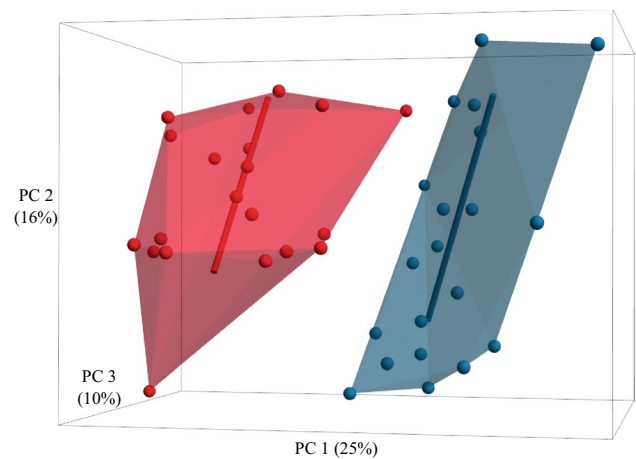
Fig. 4 3D shape space of Procrustes shape variables (PC1-3). Modern Eurasian wolves (red) and modern mesaticephalic dogs (blue). The central line in each convex hull depicts the dog and wolf trajectories of allometry in the 3D shape space

The most pronounced shape difference involves the relative size of the lateral semicircular canal, being distinctly larger in modern dogs, based on a posterior-medial extension (Fig. 6). Wolves reveal slightly larger vertical semicircular canals, resulting from a superior elongation of the common crus (the part/limb shared by the anterior and posterior semicircular canal). The posterior semicircular canal in wolves shows more torsion, whereas in dogs it runs more planar. The slightly larger oval window in wolves is oriented more laterally than in dogs. Finally, relative cochlea streamline length is longer in wolves, adding approximately one-third of a turn. Relative to the caudal vestibular portion, the more rostral central bony axis of the cochlea (the modiolus), housing the cochlear nerve and the spiral ganglion, is tilted slightly more anteroventrally in dogs, compared to wolves (Fig. 6).

Discussion

We found significant differences between bony labyrinth mean shapes of modern wolves and similar-sized modern dogs, resulting in non-overlapping clusters in shape space. Bony labyrinth shape thus allows clear separation between the two sub-species.

The total amount of variation in the shape of the bony labyrinth was similar in modern dogs and wolves (Schweizer et al. 2017). This result is confirmed by our study, although we used a different landmark protocol (Gunz et al. 2012). This equality of variance likely results from the relatively conserved configuration of the bony structures surrounding the labyrinth. Indeed, housed inside the petrous bone, the bony labyrinth is part of the basicranium, a region known to

Fig. 3 Box-plot showing the distribution of centroid size (displayed on the *y* axis) of Procrustes shape variables of the bony labyrinths of modern mesaticephalic dogs and modern Eurasian wolves showing the on average slightly larger bony labyrinths of the latter group

Fig. 5 2D shape space of Procrustes shape variables (PC1 vs. PC2 and PC1 vs. PC3). Modern Eurasian wolves (red) and modern mesaticephalic dogs (blue). The central line in each convex hull depicts the dog and wolf trajectories of allometry in the 2D shape space. Bony labyrinth shape changes related to the individual PC axes are visualized three standard deviations away from the mean, in negative (gray) and positive (red) direction. All shape changes are visualized in lateral and superior view for the first three PC axes
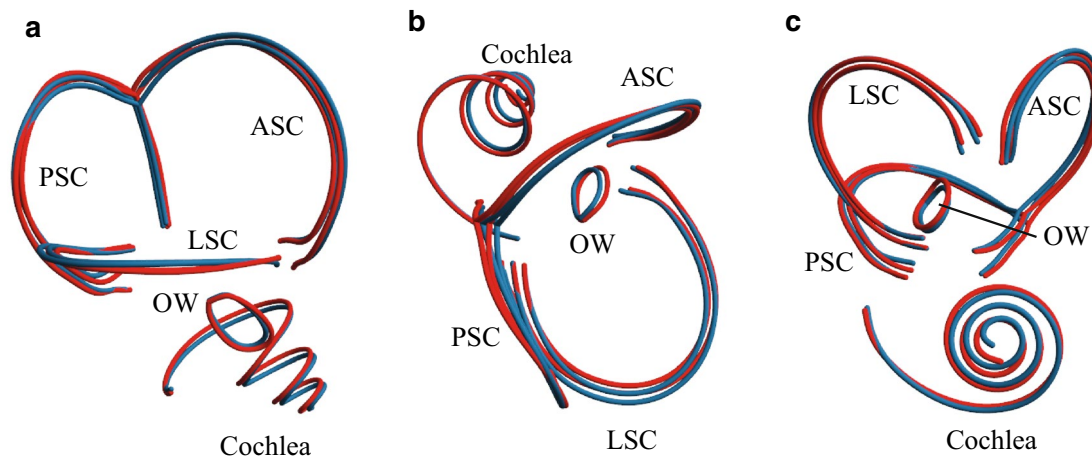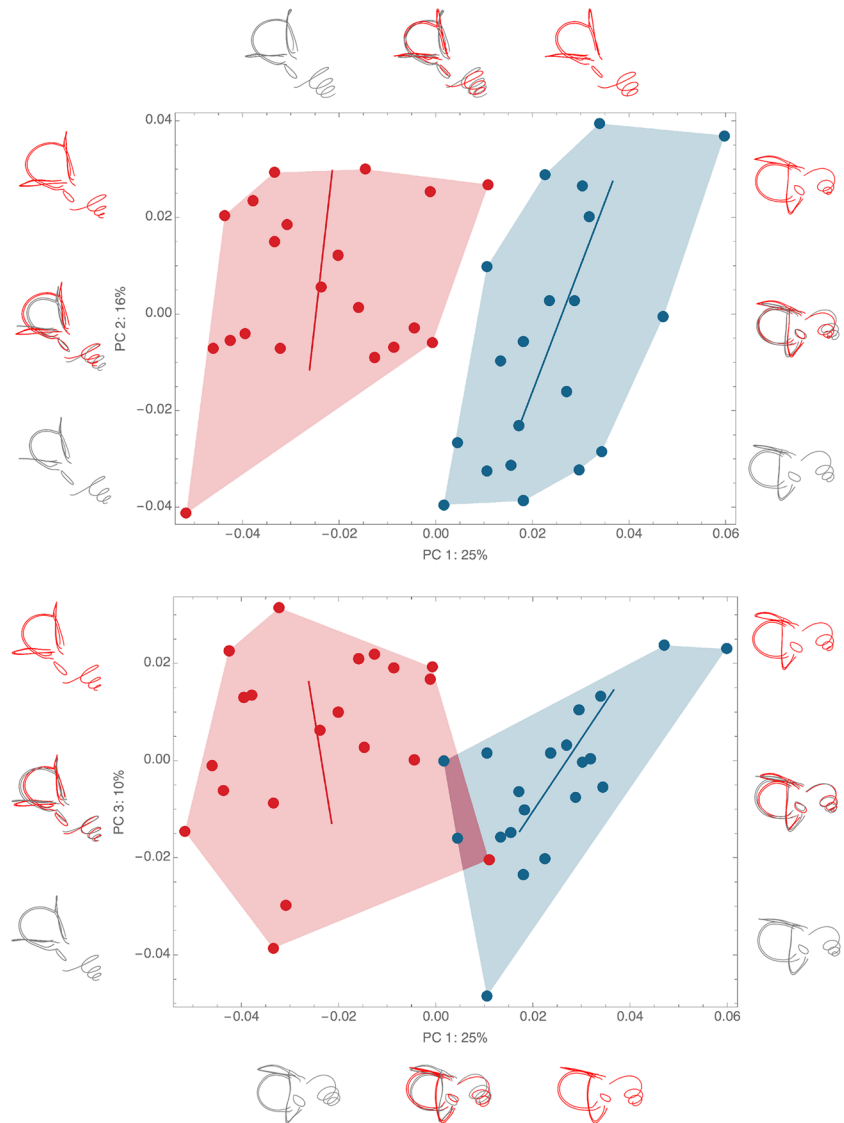
Fig. 6 Mean shapes of modern Eurasian wolves (red) and modern mesaticephalic dogs (blue) in lateral (**a**), superior (**b**), and oblique, ventrolateral (**c**) view. *ASC* anterior semicircular canal, *PSC* osterior semicircular canal, *LSC* lateral semicircular canal, *OW* oval window

show less anatomical variation compared to other parts of the canine skull (Lüpz 1974). Since shape of the mammalian bony labyrinth has been shown to co-vary with aspects of the remaining basicranium (Spoor and Zonneveld 1998; Gunz et al. 2013), it is likely that dog vs. wolf variation in labyrinth shape relates to constraints imposed by developmental integration within the cranial skull base of modern dogs and wolves. This developmental differentiation should be present prenatally (as development of the bony labyrinth is completed before birth), and not based on postnatal ontogenetic diversity occurring during growth (Wayne and Vilà 2001; Jeffery and Spoor 2004; Costeur et al. 2017; Geiger et al. 2017). Shape variances between dogs and wolves suggest that there is no relaxed stabilizing selection on the canine bony labyrinth, as the result of domestication (Perier et al. 2016). However, relaxed stabilizing selection would be expected in domesticated wolves (dogs), based on reduced natural selection pressure (e.g. bright coat color survivors that are not present in the wild); reduced food stress (anthropogenic food sharing and feeding); and reduced intra- (other wolf pack conflicts as the main death cause in wolves) and inter-species (e.g., bears) carnivore competition.

Centroid size of the labyrinth is significantly smaller among our modern dog sample, implying a smaller overall labyrinth size, despite congruence of cranial size. Correlation between inner ear size and brain volume might be an underlying explanation, as brain volume ratio is smaller in dogs compared to similar-sized wolves (Kruska 1986, 1988a, b; Geiger and Haussman 2016). Brain size reduction (about 25%) is typical for domesticates (Arbuckle 2002; Zeder et al. 2006; Zeder 2012), and is the result of the reduced stress, related to the anthropogenic environment (Hemmer 1973; Zeder 2012). Brain size reduction is not a general phenomenon but caused by reduction of specific brain structures, localized specifically in the metencephalon, specifically the reticulo-activated system (RES) (Boitani and Ciucci 1995; Kruska 1988a). This region also houses the brain nuclei innervating the labyrinth. As a result of this selective brain size reduction, there is reduced hypothalamic-adrenocorticotropic hormone production and secondary reduced adrenal glucocorticosteroid production (Arbuckle 2002; Belyaev et al. 1985; Hemmer 2005; Trut et al. 2009).

Shape differences between bony labyrinths of wolves and modern dogs do not result from differences in overall labyrinth size since the species segregate by shape changes along PC 1, which is affected only weakly by allometry (4% of variance explained by PC 1). Hence, shape differences between wolf and dog labyrinths must result from other factors. Simple correlations between vestibular bony labyrinth shape and function of the inner ear have been disputed (David et al. 2016), and the contribution of vestibular functional factors to shape variation cannot be tested at present. Similar concerns apply to the functional shape of the cochlea (Manoussaki et al. 2008; Pietsch et al. 2017). Since sensory capacities of most dog breeds and wolves are thought to be similar (Scott 1950), shape changes in the canine labyrinth affecting mostly lateral canal size and cochlea shape could represent a response to the need of maintaining (instead of altering) similar auditory and vestibular functions relative to absolute size differences between inner ears of modern wolves and modern dogs. Given the close relationship between cranial base morphology and bony labyrinth shape in other mammals (Spoor and Zonneveld 1998; Jeffery and Spoor 2004; Gunz et al. 2013), it appears likely that shape disparity may relate mainly to spatial constraints (Pietsch et al. 2017) or differences in neurocranial developmental integration.

Our data suggest that bony labyrinth shape is a neomorphic feature of modern dog anatomy that allows differentiation of modern wolves and modern dogs. Possibly, these observations were obscured in earlier studies by allometric effects resulting from the large size range among modern dogs (Schweizer et al. 2017). The ability to differentiate modern dogs and wolves with similar skull lengths demonstrates that bony labyrinth shape is a viable taxonomic marker.

Conclusion

In modern Eurasian wild wolves and modern mesaticephalic dogs of comparable skull length, the inner ear differs statistically in: centroid size (smaller in dogs); relative size of the lateral semicircular canal (larger in dogs); relative size of the vertical canal (smaller in dogs); and is less twisted, more planar in form in the vertical canal (dogs). Relative size of the oval window and cochlea streamline length also differ (smaller in dogs), and the modiolus is tilted anteroventrally in dogs. Based on these differences, inner ears of similar sized modern dogs and modern wolves can be differentiated with certainty.

Compliance with ethical standards

Conflict of interest There are no conflicts of interest for any of the authors.

Ethical approval No animals were involved, skulls were from existing collections. No humans were involved.

Human and animal rights statement This article does not contain any studies with human participants or animals, performed by any of the authors.

References

Aggarwal R, Kivisild T, Ramadevi J, Singh L (2007) Mitochondrial DNA coding region sequences support the phylogenetic distinction of two Indian wolf species. J Zool Sys Evol Res 45:163–172

Alloing-Séguier L et al (2013) The bony labyrinth in diprotodontian marsupial mammals: diversity in extant and extinct forms and relationships with size and phylogeny. J Mamm Evol 20:191–198

Ameen C et al (2017) A landmark-based approach for assessing the reliability of mandibular tooth crowding as a marker of dog domestication. J Archaeol Sci 85:41–50

Arbuckle BS (2002) Experimental animal domestication and its application to the study of animal exploitation in prehistory. In: Vigne J-D (ed) International conference of archaeozoology. Oxbow books, Durham, pp 18–33

Belyaev DK, Plyusnina IZ, Trut LN (1985) Domestication in the silver fox (Vulpes Fulvus Desm): Changes in physiological boundaries of the sensitive period of primary socialization. Appl Anim Behav Sci 13:359–370

Boitani L, Ciucci P (1995) Comparative social ecology of feral dogs and wolves. Ethol Ecol Evol 7:49–72

Bookstein F (1997) Morphometric tools for landmark data: geometry and biology. Cambridge University Press, Cambridge

Costeur L et al (2017) Prenatal growth stages show the development of the ruminant bony labyrinth and petrosal bone. J Anat 230:347–353

David R et al (2016) Assessing morphology and function of the semicircular duct system: introducing new in situ visualization and software toolbox. Sci Rep 6:32772

de León MS et al (2018) Human bony labyrinth is an indicator of population history and dispersal from Africa. PNAS 115:4128–4133

Drake A, Klingenberg C (2010) Large-scale diversification of skull shape in domestic dogs: disparity and modularity. Am Nat 175:289–301

Drake A, Coquerelle M, Colombeau G (2015) 3D morphometric analysis of fossil canid skulls contradicts the suggested domestication of dogs during the late Paleolithic. Sci Rep 5:8299

Drake A et al (2017) Three-dimensional geometric morphometric analysis of fossil canid mandibles and skulls. Sci Rep 7:9508

Geiger M, Haussman S (2016) Cranial suture closure in domestic dog breeds and its relationships to skull morphology. Anat Rec 299:412–420

Geiger M et al (2017) Neomorphosis and heterochrony of skull shape in dog domestication. Sci Rep 7:13443

Good P (2013) Permutation tests: a practical guide to resampling methods for testing hypotheses. Springer, New York

Gunz P, Mitteroecker P (2013) Semilandmarks: a method for quantifying curves and surfaces. Ital J Mamm 24:103–109

Gunz P, Mitteroecker P, Bookstein FL (2005) Semilandmarks in three dimensions. Modern morphometrics in physical anthropology. Springer, New York, pp 73–98

Gunz P et al (2012) The mammalian bony labyrinth reconsidered, introducing a comprehensive geometric morphometric approach. J Anat 220:529–543

Gunz P et al (2013) Morphological integration of the bony labyrinth and the cranial base in modern humans and Neandertals. PESHE 2:104

Hemmer H (1973) Zur Abstammung des Haushundes und zur Veränderun der relativen Hirngrösse bei der Domestikation. In: Zoologische Beitragen, vol 21, pp 97–104

Hemmer H (2005) Neumuhle-Riswicker Hirsche-Erste planmassige Zucht einer neuen Nutztierform. Naturwissenschaftliche Rundschau 58:255–261

Janssens L, Miller R, Van Dongen S (2016a) The morphology of the mandibular coronoid process does not indicate that Canis lupus chanco is the progenitor to dogs. Zoomorphology 135:269–277

Janssens L, Spanoghe I, Miller R, Van Dongen S (2016b) Can orbital angle morphology distinguish dogs from wolves? Zoomorphology 131:149–158

Janssens L, Verhaert L, Berkowic D, Adriaens D (2016c) A standardized framework for examination of oral lesions applied to a series of Middle)East wolf skulls (Carnivora: Canidae: Canis lupus). J Mamm 97:1111–1124

Janssens L et al (2019) An evaluation of classical morphologic and morphometric parameters reported to distinguish wolves and dogs. J Arch Sci Rep 23:501–533

Jeffery N, Spoor F (2004) Prenatal growth and development of the modern human labyrinth. J Anat 204:71–92

Kruska D (1986) How fast can total brain size change in mammals? J Hirnforsch 28:59–70

Kruska D (1988a) Effects of domestication on brain structure and behavior in mammals. Human Evol 3:473–485

Kruska D (1988b) Mammalian domestication and its effect on brain structure and behavior. Intelligence and evolutionary biology. Springer, New York, pp 211–250

Lam Y, Chen X, Pearson O (1999) Intertaxonomic variability in patterns of bone density and the differential representation of bovid, cervid, and equid elements in the archaeological record. Am Antiq 64:343–362

Lam Y, Pearson O, Marean CW, Chen XJ (2003) Bone density studies in zooarchaeology. J Archaeol Sci 30:1701–1708

Lebrun R, De León M, Tafforeau P, Zollikofer C (2010) Deep evolutionary roots of strepsirrhine primate labyrinthine morphology. J Anat 216:368–380

Lüpz P (1974) Biometrische Untersuchungen an den Schädelbasis des Haushundes. Zool Anzeitungen 192:383–413

Lyman R (1984) Bone density and differential survivorship of fossil classes. J Anthropol Archaeol 3(4):259–299

Manoussaki D et al (2008) The influence of cochlear shape on low-frequency hearing. PNAS 105:6162–6166

Masschaele B et al (2013) A 240 kV micro-CT setup optimized for research. J Phys Conf Ser 463:012012 **(IOP Publishing)**

Mitteroecker P, Gunz P (2009) Advances in geometric morphometrics. Evol Biol 36:235–247

Nummela S (1995) Scaling of the mammalian middle ear. Hear Res 85:18–30

Perier A, Lebrun R, Marivaux L (2016) Different level of intraspecific variation of the bony labyrinth morphology in slow-versus fast-moving primates. J Mamm Evol 23:353–368

Pietsch M et al (2017) Spiral form of the human cochlea results from spatial constraints. Sci Rep 7(1):7500

Rohlf F (1990) Morphometrics. Ann Rev Ecol Syst 21:299–316

Rohlf F, Marcus LF (1993) A revolution morphometrics. Trens Ecol Evol 8:129–132

Schweizer A et al (2017) Size variation under domestication: conservatism in the inner ear shape of wolves, dogs and dingoes. Sci Rep 7:13330

Scott J (1950) The social behavior of dogs and wolves: an illustration of sociobiological systematics. Ann N Y Acad Sci 51:1009–1021

Slatter D (2003) Textbook od small animal surgery. Saunders, Philadelphia

Spoor F, Zonneveld F (1998) Comparative review of the human bony labyrinth. Am J Phys Anthropol 107:211–251

Spoor F et al (2007) The primate semicircular canal system and locomotion. PNAS 104:10808–10812

Thalmann O et al (2013) Complete mitochondrial genomes of ancient canids suggest a European origin of domestic dogs. Science 342:871–874

Trut L, Oskina I, Kharlamova A (2009) Animal evolution during domestication: the domesticated fox as a model. BioEssays 31:349–360

Von den Driesch A (1976) A guide to the measurement of animal bones from archaeological sites: as developed by the: Institüt fur Palaeoanatomy, Domestikanzionsforschung und Geschichte der Tiermedizin, University Munich. Cambridge Peabody Museum Press, Cambridge

Wayne R, Vilà C (2001) Phylogeny and origin of the domestic dog. Genet Dog 1:13–21

Zeder M (2012) The domestication of animals. J Anthropol Res 68:161–190

Zeder MA, Emshwiller E, Smith BD, Bradley DG (2006) Documenting domestication: the intersection of genetics and archaeology. Trends Genet 22:139–155